^{8}Be+^{8}Be decay of excited states in ^{16}O

M. Freer, M. P. Nicoli, and S. M. Singer
School of Physics and Space Research, University of Birmingham, Edgbaston, Birmingham B15 2TT, United Kingdom

C. A. Bremner, S. P. G. Chappell, W. D. M. Rae, and I. Boztosun*
Nuclear and Astrophysics Laboratory, University of Oxford, Keble Road, Oxford OX1 3RH, United Kingdom

B. R. Fulton, D. L. Watson, B. J. Greenhalgh, G. K. Dillon, and R. L. Cowin
Department of Physics, University of York, Heslington, York YO10 5DD, United Kingdom

D. C. Weisser
Department of Nuclear Physics, The Australian National University, Canberra ACT 0200, Australia
(Received 17 August 2004; published 14 December 2004)

The ^{12}C(^{12}C,^{8}Be+^{8}Be)^{8}Be reaction has been studied with 18 beam energies from 82 to 120 MeV. The detection of four of the six final-state α-particles in an array of eight 16-element strip detectors permitted the full reconstruction of the reaction kinematics. ^{16}O excitation energy spectra spanning 19–40 MeV were measured, which provided evidence for ^{16}O excited states up to 35.1 MeV. Angular correlation analysis indicates the dominant spins are 6 and 8 $\hbar$, possibly extending to 10 $\hbar$ at the highest excitation energies. The resulting energy-spin systematics are compared with the predictions of the α cluster model and cranked Nilsson-Strutinsky calculations.

DOI: 10.1103/PhysRevC.70.064311 PACS number(s): 25.70.Ef, 25.70.Mn, 27.20.+n

I. INTRODUCTION

The study of nuclei at high excitation offers a considerable challenge. With exponential growth in level densities, the single-particle spectrum becomes increasingly complex. The study of decay channels which require the emission of correlated particles can limit the spectral density and, moreover, provide a signature for states with a special character, e.g., a cluster structure.

The ^{16}O nucleus has long been identified with α-clustering, dating back to the earliest days of the subject [1], and more recently descriptions of the various rotational bands in terms of the geometric arrangements of the α-particle constituents have been found [4]. The α cluster model is, however, not the only model which provides an effective description of this nucleus. Other approaches include the shell model approach, Hartree-Fock approaches [2,3], and the cranked Nilsson-Strutinsky approach [5]. The most exotic structures predicted by such models are those described by 8p-8h configurations, which in the α-cluster model limit corresponds to an elongated α-particle arrangement. Such states are broadly predicted to exist close to the 4α-decay threshold, a region which has met with considerable interest due to the possible existence of states described by a dilute gas of α-particles [6].

The 8p-8h states might be expected to decay strongly to the ^{8}Be+^{8}Be final state, the detection of which is a considerable experimental challenge, given that such a decay process results in four final-state particles. Nevertheless, there has been some experimental progress in this direction. Chevalier *et al.* [7] made a study of the ^{12}C(α,^{8}Be)^{8}Be reaction using two small silicon detectors to identify the ^{8}Be decay. However, the advent of strip detectors has allowed such multiparticle final states to be detected with far greater sensitivity. Wuosmaa [8] made a measurement of the ^{12}C(^{12}C,^{8}Be+^{8}Be) reaction which provided some limited evidence for the decay of ^{16}O excited states, and, finally, a measurement of the ^{12}C(^{16}O,4α) reaction has also been performed [9].

However, the data on the ^{8}Be decay channel remain extremely limited, and to test structural models a far greater survey is required. In the present paper, we present a comprehensive series of measurements of the ^{12}C(^{12}C,^{8}Be +^{8}Be) reaction spanning ^{16}O excitation energies from 19 to 40 MeV.

II. EXPERIMENTAL DETAILS

The present measurements were performed at the Australian National University (ANU). The experiment was conducted using the Charissa strip detector array located in the MEGHA chamber [10]. The array was composed of eight 500 μm, 50×50 mm^2 Si strip detectors. These covered an angular range of $\theta_{lab}=5°-60°$, and an azimuthal angular range of $\Delta\phi\approx100$ degrees on each side of the beam axis, as shown in Fig. 1 of Ref. [11]. Each strip detector was divided into 16 position-sensitive strips, with the position-sensitive axis orientated towards the beam axis.

^{12}C beams, with an intensity of 50 enA, and energies ranging from $E_{beam}=82$ to 120 MeV, were incident upon a 60 μg cm^{-2} ^{12}C target foil. The higher beam energies

*Department of Physics, Erciyes University, 38039 Kayseri, Turkey.

($E_{beam} > 99$ MeV) were obtained using the linear accelerator in conjunction with the pelletron tandem 14UD accelerator. Due to the large beam energies used and the limited detector thickness, some events which produced α-particles with an energy in excess of $\sim$32 MeV experienced punch-through (i.e., the α-particles did not stop in the silicon detectors) and thus only a fraction of the α-particle energy was deposited within the detector. Such processes contributed to the overall background levels observed at the higher energies. However, the reconstruction methods employed in the analysis were able to clearly distinguish the punch-through events, suppressing this contribution. The corresponding loss of acceptance was accounted for using the Monte Carlo simulations of the reaction and detection processes. The energy response of the detection system was calibrated using elastic scattering of ^{12}C ions from both ^{197}Au and ^{12}C targets.

III. ANALYSIS AND RESULTS

The large angular coverage of the detection system and the high segmentation is ideally matched to high multiplicity final states and provides a very effective filter of such reaction processes. In the case of the $^{12}C(^{12}C, ^{16}O^* \rightarrow {}^8Be + {}^8Be){}^8Be$ α-transfer reaction, the final state naturally consists of 6α-particles given that all the low-lying states in ^{8}Be are unbound to α-decay. However, it is possible to reconstruct the complete reaction process through the detection of only four of the six particles. The measurement of the energy and angle of each detected particle, coupled with an assumption that such events correspond to the detection of mass 4 nuclei, allows the reconstruction of the momentum and thus energy of the unobserved ^{8}Be recoil.

However, the first stage in the analysis was to reconstruct the relative energies of pairs of particles to determine if two ^{8}Be nuclei were produced in the final state. The α-α relative energy is given by

$$E_{rel} = \frac{1}{2}\mu|\mathbf{v}_{\alpha 1} - \mathbf{v}_{\alpha 2}|^2, \tag{1}$$

where $\mathbf{v}_{\alpha 1,2}$ are the vector velocities of the two selected α-particles and μ is their reduced mass.

The result of this reconstruction is shown in Fig. 1.

There is a strong peak at 96 keV, with a full width at half maximum (FWHM) of 38 keV, which would correspond to the decay of the ^{8}Be ground state (92 keV). The close correspondence between the measured energy and the calculated decay energy taken together with the narrow peak width is an indication that all eight of the detector responses are well matched and accurately calibrated.

This unambiguous signature for the decay of the ^{8}Be ground state was used to select events in which two pairs of the four particles corresponded to the decay of two ^{8}Be ground states. This was done by calculating the relative energy for every combination of two particles and then determining if the relative energy was within the peak shown in Fig. 1. Following the identification of the decay of two ^{8}Be nuclei, it is possible to apply the principles of momentum conservation to deduce the momentum, and thus energy

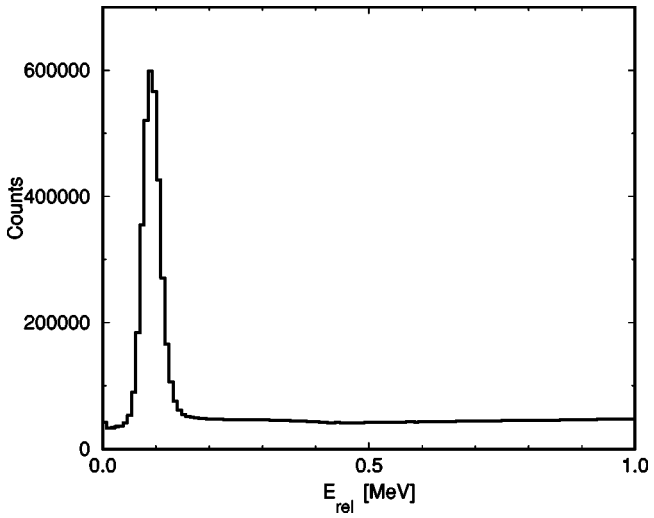

FIG. 1. The relative energy spectrum for pairs of hits for multiplicity 4 events, calculated assuming all four detected particles have $A=4$.

(E_{recoil}), of the unobserved recoil, assuming that the recoil was produced as a single entity, as would be expected in an α-transfer reaction.

The total energy spectrum is calculated as

$$E_{tot} = E_{beam} - E_{recoil} - \sum_{i=1}^{4} E_{\alpha i} \tag{2}$$

and is shown plotted in Fig. 2. The Q-value for the $^{12}C(^{12}C, 4\alpha){}^8Be$ reaction is -14.637 MeV, and thus for a beam energy (E_{beam}) of 116.4 MeV the ^{8}Be recoil ground state should appear at 101.76 MeV. The highest-energy peak in the present spectrum appears at 102.6 MeV, i.e., within 1 MeV of that calculated. The magnitude of this discrepancy

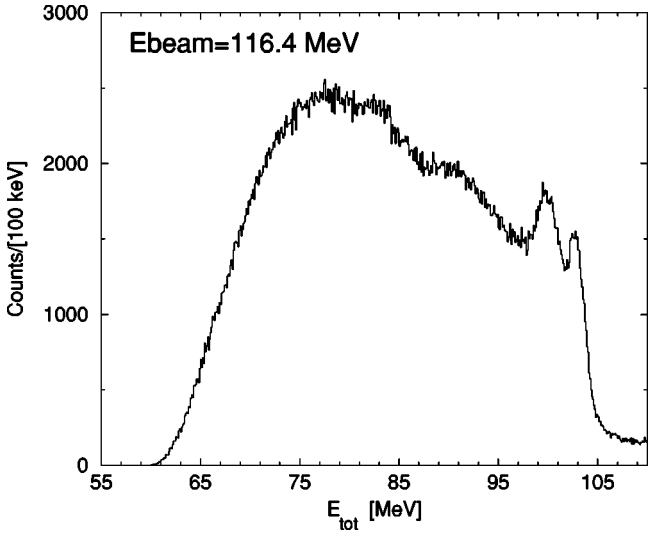

FIG. 2. The total energy spectrum corresponding to the $^{12}C(^{12}C, 4\alpha){}^8Be$ reaction, gated on two pairs of the four detected α-particles being produced from the decay of $^8Be_{gs}$. The present spectrum corresponds to a beam energy of 116.4 MeV.

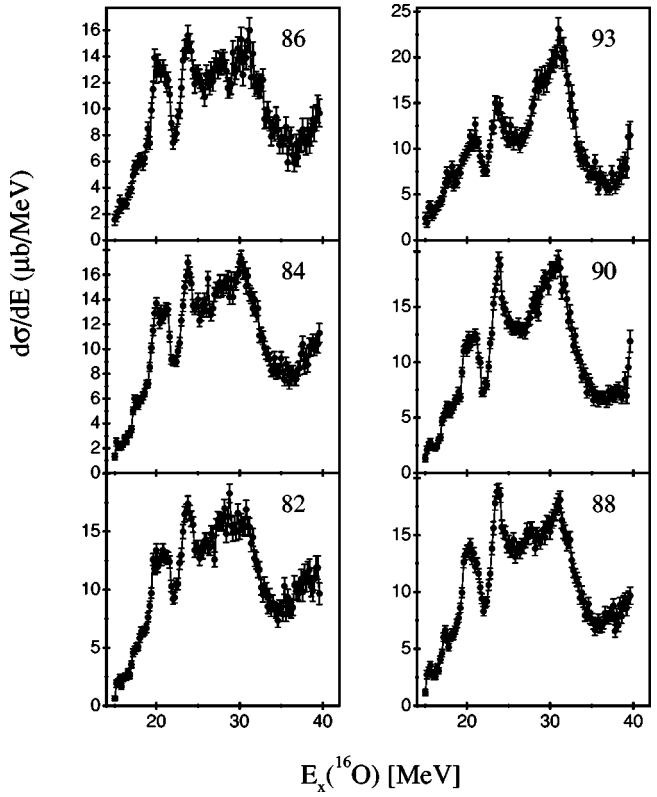

FIG. 3. The ^{16}O excitation energy spectra reconstructed from decays to ^{8}Be+^{8}Be for beam energies 82–93 MeV.

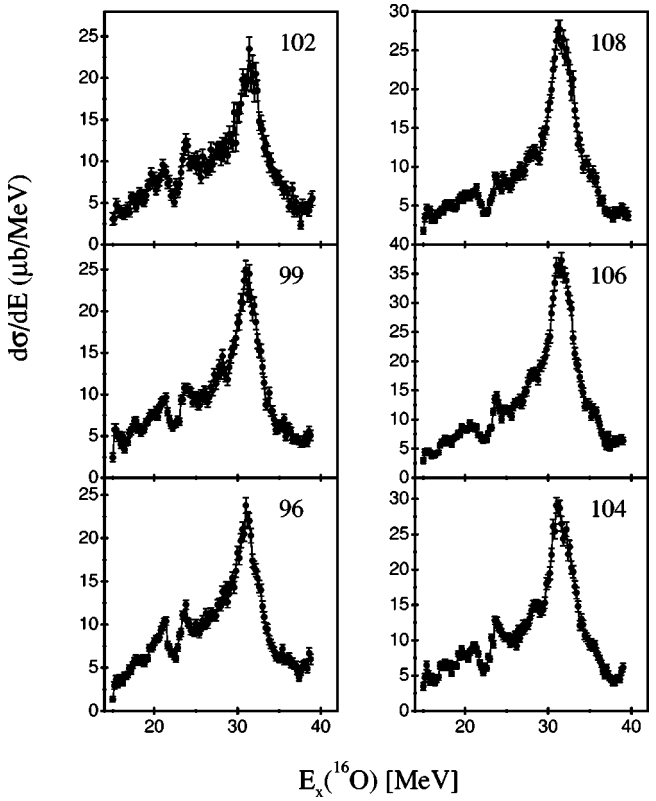

FIG. 4. The ^{16}O excitation energy spectra reconstructed from decays to ^{8}Be+^{8}Be for beam energies 96–108 MeV.

was typical across the range of beam energies performed in these measurements. Given that the calibration was performed with ^{12}C ions rather than α-particles, such uncertainties in the calculated energies are reasonable. The reconstructed total energy resolution extracted from the width of the highest energy peak is 1.66 MeV.

A further peak is evident at an energy of 2.8 MeV lower in total final-state energy, which would correspond to the ^{8}Be first excited state (3.1 MeV, 2^{+}), and there is some evidence for the 11.35 MeV, 4^{+}, state close to a total energy of 91 MeV. The total energy spectrum thus demonstrates that the ^{12}C(^{12}C, ^{16}O$^{*}\rightarrow{}^{8}$Be+^{8}Be)^{8}Be reaction is observed in the present data.

A. ^{16}O excitation energy spectra

By selecting the events lying within the highest-energy peak in the excitation energy spectrum, a 3 ^{8}Be$_{gs}$ final-state results. The ^{16}O excitation energy spectra corresponding to the decay into the two detected ^{8}Be nuclei were then reconstructed. The majority of these events correspond to the two ^{8}Be nuclei being detected on opposite sides of the beam axis, in other words small ^{16}O center-of-mass emission angles. The resulting excitation energy spectra are shown in Fig. 3–5, and have been normalized for the target thickness, beam exposure, and detection efficiency. The excitation energy spectra corresponding to events leading to the decay of ^{16}O into one of the detected ^{8}Be nuclei and the undetected ^{8}Be were reconstructed, but these showed minimal evidence for ^{16}O excitations.

The detection efficiencies were calculated based upon the energy and angular acceptances of the detection system and using Monte Carlo simulations of all stages of the reaction process leading to the production of the four α-particles. The particles produced in the decay process were simulated using isotropic emission whilst the primary angular distribution governing the emission of the excited ^{16}O nucleus was assumed to be exponential in form in the center-of-mass system. The detection efficiencies rose from 0% at 14 MeV excitation energy to 10–15 % at 20 MeV, falling to 3–5 % at an excitation of 40 MeV. The efficiency profiles were a smooth function of excitation energy, and thus structure in the excitation energy spectra cannot be attributed to their behavior.

The excitation energy spectra extend from the decay threshold at ~15 MeV up to ~40 MeV and show a structure which evolves strongly with the center-of-mass energy of the target-projectile system. At lower center-of-mass energies, the lower excitations are emphasized, whilst the highest-energy states are most prominent for the largest collision energies. The spectra are clearly complex, but the dominant features remain remarkably constant in excitation energy as a function of beam energy. For example, the peak observed at 23.6 MeV in the majority of the spectra shifts by less than 200 keV (each data bin being 200 keV wide) from beam energies ranging from 82 to 106 MeV. This indicates that there are few residual dependencies in the calibrations of the detectors which affect the excitation energy spectra.

A closer look at the spectra indicates that the prominent excited states appear at energies of 17.7, 20.0, 21.2, 23.6,

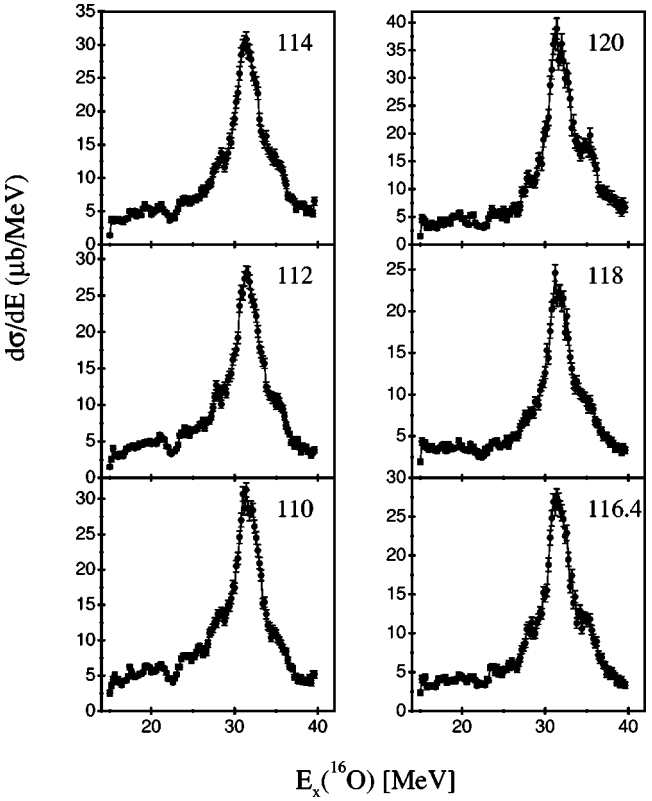

FIG. 5. The ^{16}O excitation energy spectra reconstructed from decays to ^{8}Be+^{8}Be for beam energies 110–120 MeV.

(25.0), 27.6, 28.8, 31.1, 32.6, and 35.1 MeV. The 17.7 MeV is observed as a shoulder in most of the spectra in Fig. 3, and is most clearly observed in the E_{beam}=93 MeV data. The 20.0 and 21.2 MeV peaks appears as a doublet again in Fig. 3 and notably the relative strength of the two states changes with beam energy. The 23.6 MeV peak is observed strongly in most spectra and appears to have a high-energy shoulder at 25.0 MeV, particularly evident in the E_{beam}=88 MeV data. There are probably a number of states contributing between 26 and 29 MeV, but the E_{beam}=86 and 93 MeV data suggest peaks at 27.6 and 28.8 MeV. Finally all of the higher beam energy spectra show a strong peak at ~31.5 MeV, but the shape of the peak in many of the spectra, e.g., the E_{beam} =104, 106, and 108 MeV data, suggests that this may be an unresolved doublet with peaks at 31.1 and 32.6 MeV. Finally, in the 120 MeV data there is a strong peak at 35.1 MeV which has gradually grown in intensity with increasing beam energy.

An upper limit for the excitation resolution may be judged from the width of the 23.6 MeV state, which has a width of 1.2 MeV. It would appear that the natural widths of states are less than this in most cases. This resolution is dominated by the precision with which it is possible to measure the position of the incident particles in the silicon strip detectors, 0.5–1 mm depending on the incident energy. Given this resolution and the changing peak profiles, the data suggest that the full complexity of the excitation energy spectra is not revealed here, and higher-resolution measurements would be of benefit.

B. Angular correlations

Given that both the initial and final states contain exclusively spin zero particles, then it is possible to utilize the technique of angular correlations to extract the spins of the observed states [12]. Furthermore, since the decay is into two identical spin-zero bosons, the present spectrum of states must be limited to even spin and even parity.

In the present reaction, there are two center-of-mass systems, that corresponding to the $^{12}C+^{12}C\rightarrow^{16}O^{*}+^{8}Be$ α-transfer reaction, which may be described in terms of the two angles θ^* and ϕ^*, and the second being the subsequent decay into two ^{8}Be nuclei, described by the angles ψ and χ (as detailed in Ref. [12]). The angles θ^* and ψ are the polar angles measured with respect to the beam axis and measure the center-of-mass emission angle of the ^{16}O ejectile and the inclination of the ^{8}Be+^{8}Be relative velocity vector.

Typically, for reactions involving spin-zero initial- and final-state particles, the number of reaction amplitudes is small and the correlations observed between the two angles θ^* and ψ take the form of a sloping ridge pattern. The periodicity of the ridges is described by a Legendre polynomial of order of the spin of the decaying state, i.e., $P_J(\cos\psi)$. As the dominant orbital angular momenta in the reaction are those corresponding to grazing trajectories, the gradient of the ridges is given by the ratio of the exit channel grazing angular momentum to the spin of the state populated,

$$\frac{\Delta\theta^*}{\Delta\psi}=\frac{J}{l_f}=\frac{J}{l_i-J}, \tag{3}$$

where l_i and l_f are the initial- and final-state grazing angular momenta. If the "stretched" configuration dominates, which is typically the case for such reactions (see [12] and references therein), then the entrance and exit channel angular momenta can be related via the expression $l_f=l_i-J$.

The angular correlations therefore provide two signatures of the spin of the decaying ^{16}O state. The periodicity yields a value for J, which should correlate with that extracted from the ridge gradient, assuming l_i is known. In addition, the value of J extracted from the periodicity should provide a consistent value of l_i for all of the correlations. Figures 6–10 show the projection of the two-dimensional θ^*-ψ correlations, along the ridge locii, onto the $\theta^*=0$, ψ axis. The angle of projection is selected that maximizes the peak-to-valley ratio. In this way, the periodicity of the correlations can be compared with the functions $P_J(\cos\psi)$ in order to extract the spin J of each states.

Figure 11 shows the sum of all of the excitation energy spectra for the 18 beam energies without efficiency correction. Also displayed are the 12 data bins (labeled A–L) for which the angular correlation data were analyzed. Typically, the correlation phase space was much larger in the case of the lower beam energies and thus the range in ψ was more extensive. The phase space is limited by the angular acceptance of the detectors and the detection energy limits, including punch-through effects. This modifies the intensity variation of the projected correlations as a function of ψ, but not the periodicity of the correlation pattern.

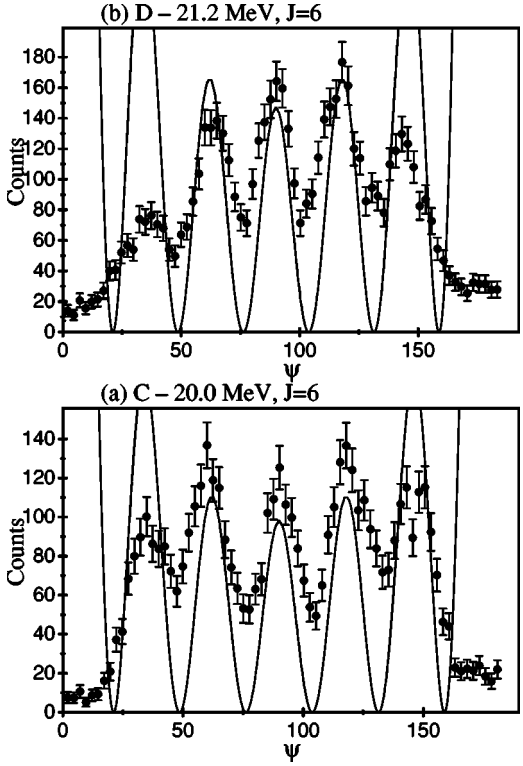

FIG. 6. The projected angular correlations for the two states at (a) 20.0 MeV and (b) 21.2 MeV, corresponding to the gates in Fig. 11 C and D, respectively. The data correspond to the summed data for the beam energies 82 and 84 MeV. The experimental data are shown compared with Legendre polynomials of order 6, and thus indicate $J=6$ assignments.

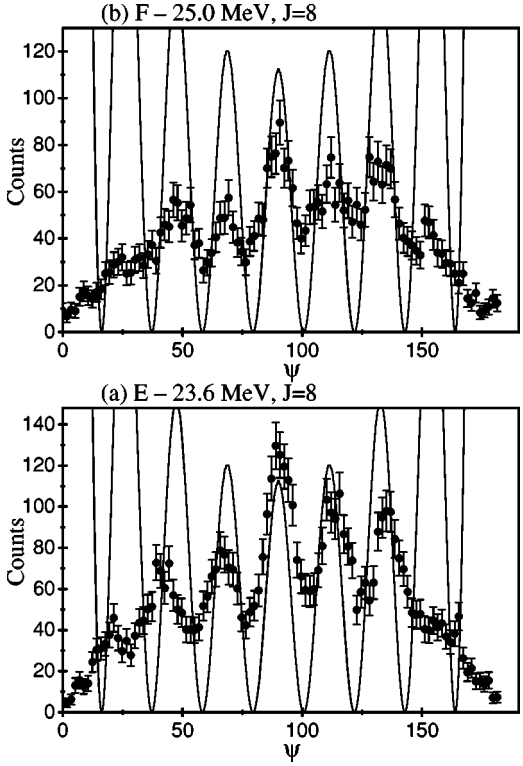

FIG. 7. The projected angular correlations for the two states at (a) 23.6 MeV and (b) 25.0 MeV, corresponding to the gates in Fig. 11 E and F, respectively. The data correspond to the summed data for the beam energies 86–90 MeV for (a) and 82 and 84 MeV for (b). The experimental data are shown compared with Legendre polynomials of order 8, and thus indicate $J=8$ assignments.

In order to enhance the statistical significance of the data, the correlations from ranges of beam energies were combined as follows: (82,84), (86,88,90), (93,96,99), (102,104,106), (108,110,112), and (114,116,118,120). In the case of the correlations corresponding to bins A and B, no strong pattern could be discerned and thus no angular momentum information could be extracted. For the data bins C-K, the correlation structure was clear and unambiguous spin assignments could be made (see Table I). In all cases, identical spins were extracted for at least three of the beam energy combinations shown above.

As noted above, the projection angle, i.e., the gradient of the correlation pattern, may be used to extract the entrance channel grazing angular momentum, l_i. The uncertainty in the extraction of the gradient of the correlation pattern thus leads to an uncertainty in the corresponding value of l_i of $\pm 1\hbar$. Given this uncertainty, all of the grazing angular momenta extracted for each beam energy combination agree within this limit. The mean values of l_i for the various beam energies are shown in Table II. As expected, there is a systematic increase in the values of l_i with increasing beam energy.

Finally, the correlation for the 35.1 MeV (data bin L) state appears to be systematically different from that of the neighboring 8^+ states, but the statistics and phase space are much more limited, the latter particularly for the higher beam energies. In this instance, the data from all beam energies have been combined, and in order to nullify the fact that the gradient changes as a function of the collision energy, only data within the region $0 \geqslant \theta^* \geqslant 3$ have been used in the analysis of the periodicity of the correlation pattern. The result is shown in Fig. 10(b). The structure indicates that the state may possess a spin of $J=10$, particularly the enhancement close to $\psi=122$ degrees.

IV. DISCUSSION

The present data permit an analysis of the energy dependence of the excitation process. There are three prominent peaks in the excitation energy spectra: (i) at 20.6 MeV corresponding to the 20.0 and 21.2 states (6^+), (ii) the 23.6 MeV state (8^+), and (iii) the peak at $\sim$32 MeV, corresponding to the 31.1 and 32.6 MeV states (8^+). The lowest-energy peak of these three has maximum intensity between the beam energies of 82–90 MeV, the second peak has maximum strength for 88–90 MeV, and the third peaks at the highest beam energies. There have been comprehensive studies of resonances in the ^{12}C+^{12}C system at high center-of-mass energies both through the ^{12}C+^{12}C entrance channel [11] and indirectly via reactions such as ^{12}C(^{16}O, ^{24}Mg$\rightarrow$ ^{12}C+^{12}C) [13]. These indicate that the last strong resonance in this system lies at a center-of-mass energy of 43 MeV and has been identified with a spin and parity of 22^+. It is interesting

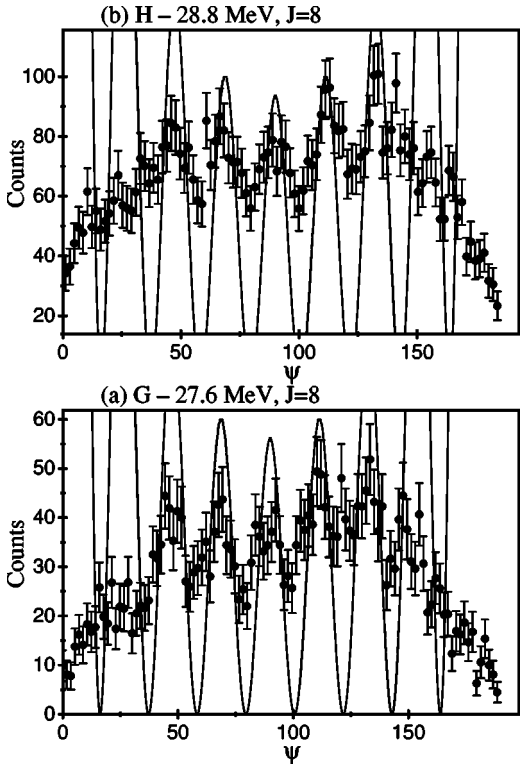

FIG. 8. The projected angular correlations for the two states at (a) 27.6 MeV and (b) 28.8 MeV, corresponding to the gates in Fig. 11 G and H, respectively. The data correspond to the summed data for the beam energies 82–84 MeV for (a) and 86 and 90 MeV for (b). The experimental data are shown compared with Legendre polynomials of order 8, and thus indicate dominant $J=8$ contributions.

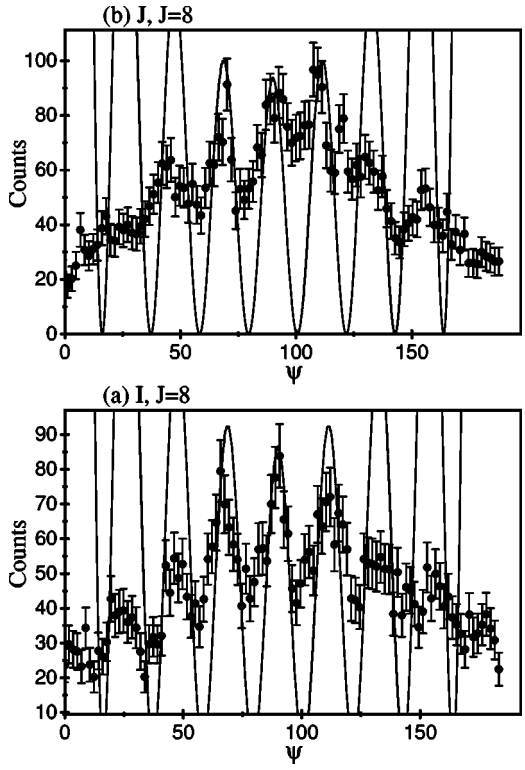

FIG. 9. The projected angular correlations in the vicinity of the 31.1 MeV peak corresponding to the gates in Fig. 11 (a) I and (b) J. The data correspond to the summed data for the beam energies 82–84 MeV for (a) and 86 and 90 MeV for (b). The experimental data are shown compared with Legendre polynomials of order 8, and thus indicate $J=8$ assignments.

that both of the two lower-energy peaks described above have an energy dependence which indicates an enhancement close to this energy, and, furthermore, the extracted value of l_i ($20.9\pm1\ \hbar$) is similar to the spin of the resonance.

However, optical model calculations indicate that the grazing angular momenta at 82, 102, and 120 MeV are 22, 24.5, and 26 $\hbar$, respectively, in rough agreement with those shown in Table II, and estimates of the angular momentum transferred by an α-particle at the grazing radius indicate that at the three beam energies, $l_{transfer}=5.7$, 6.4, and 7.0 $\hbar$, i.e., increasing by 1 to 1.5 units. In addition, calculations of the variation of the angular momentum mismatch between entrance and exit channels as a function of beam and excitation energy indicate that for a mismatch of eight units of angular momentum at a beam energy of 82 MeV, the optimal ^{16}O excitation energy is 23.5 MeV, and at 120 MeV this increases to $E_x(^{16}\mathrm{O})=28.4$ MeV. This, taken together with the increased center-of-mass phase space at the higher beam energies, may explain the shift from low spins at low ^{16}O excitation energies to higher spins at correspondingly increased values of excitation.

It would thus appear likely that the energy dependence is dominated by the dynamics of the α transfer process, rather than the existence of intermediate resonances in the ^{24}Mg nucleus, which then decays via ^{8}Be emission.

There are a number of earlier studies of the $^{12}\mathrm{C}(^{12}\mathrm{C},^{16}\mathrm{O}^{*})^{8}\mathrm{Be}$ reaction in the excitation energy range covered here, and these have tended to focus on the α-decay. For example, the studies of Sanders *et al.* [14] found a resonance at 22.5 MeV which was tentatively assigned a spin of 8, though 6 could not be excluded. An extremely comprehensive correlation analysis was reported by Rae *et al.* [15] which failed to find any 8^+ strength at 22.5 MeV, but rather close to 30 MeV, and there were indications of some very weak 10^+ strength at the upper excitation energy limit of the measurement, i.e., 32.5 MeV. The majority of the strength between 21 and 29 MeV was found to be dominated by negative-parity states 7^- and 9^-. This latter reference provides a very useful summery of the α-decay of ^{16}O in the excitation energy range 13–33 MeV.

The agreement between these earlier studies and those presented here is not strong. The α-decay channel does appear to possess some 8^+ strength close to an energy seen in the ^{8}Be decay here, and the proposed 10^+ strength seen at 32.5 MeV may be related to the 10^+ state in the present data, though the agreement is not convincing.

In the case of the ^{8}Be decay channel, there are two measurements of note: a study of the $^{12}\mathrm{C}(\alpha,^{8}\mathrm{Be})$ reaction by Chevalier *et al.* [7] and the $^{12}\mathrm{C}(^{16}\mathrm{O},4\alpha)$ reaction [9]. The first of these assigned spins and parities to the states at 16.95 MeV (2^+), 17.15 MeV (2^+), 18.05 MeV (4^+), and 19.35 MeV (6^+). A later search for an 8^+ resonance [16] using the same reaction was unsuccessful. Finally, the study of the $^{12}\mathrm{C}(^{16}\mathrm{O},4\alpha)$ reaction [9] found evidence for ^{16}O states

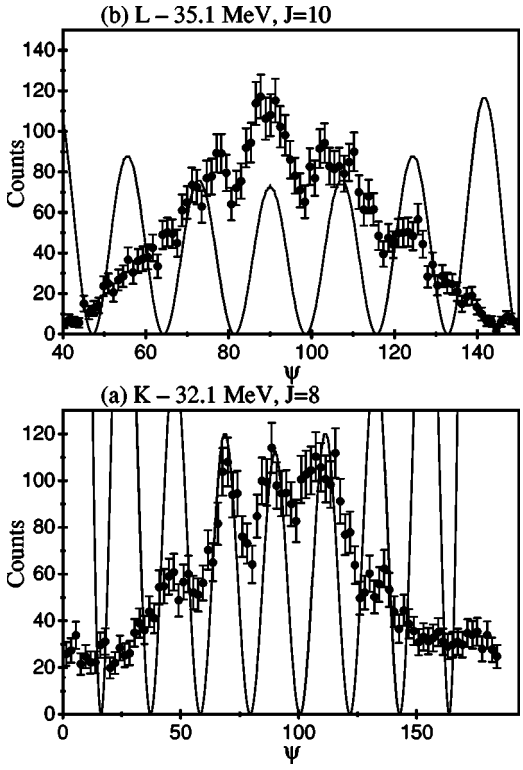

FIG. 10. The projected angular correlations for the two states at (a) 32.6 MeV and (b) 35.1 MeV, corresponding to the gates in Fig. 11 K and L, respectively. The data correspond to the summed data for the beam energies 93–99 MeV for (a) and all data for (b) but selecting only data close to $\theta^{*}=0$. The experimental data are shown compared with Legendre polynomials of order 8 and 10.

at 17.1 and 17.5 MeV with $J^{\pi}=2^{+}$, 18 MeV ($J^{\pi}=2^{+}/4^{+}$), 19.3 MeV 4^{+}, and finally 21.4 MeV, which was tentatively assigned a spin of 6. These results are shown in Table I.

It is apparent that there is little agreement between the present studies and those done previously which have examined the ^{8}Be decay channel. This is mainly related to the fact that the present yield falls significantly in the low excitation energy region. However, the 21.2 MeV 6^{+} state in the present measurement does appear to confirm the tentative assignment made for a 21.4 MeV state in Ref. [9]. However, the sum total of these measurements now provides an insight into the evolution of 8p-8h states with increasing excitation energy. Figure 12 presents the cumulative energy-spin systematics of ^{8}Be decaying ^{16}O excited states.

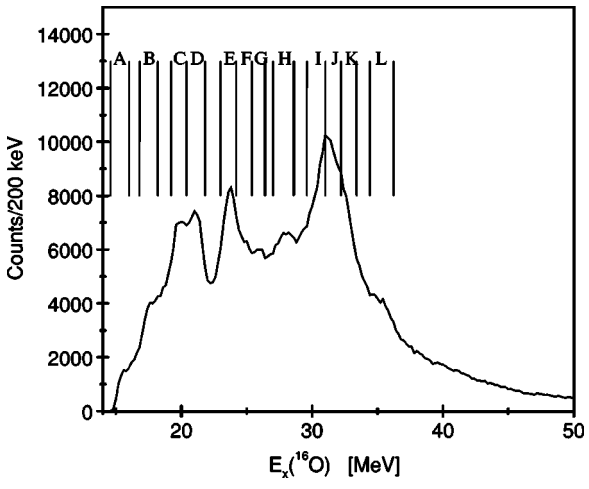

FIG. 11. The summed ^{16}O excitation energy spectra reconstructed from decays to ^{8}Be+^{8}Be for beam energies 82–120 MeV. The vertical lines indicate the limits used in the angular correlation analysis, with the intervals analyzed being labeled by the letters A–L.

TABLE I. Properties of excited states in ^{16}O from the present analysis, and those from the ^{12}C(α,^{8}Be) [7] and ^{12}C(^{16}O,4α) [9] studies. The uncertainty in the excitation energy in the present data is $<$200 keV.

Present		^{12}C(α,^{8}Be)		^{12}C(^{16}O,4α)	
E_x	J^{π}	E_x	J^{π}	E_x	J^{π}
		16.95	2^{+}		
		17.15	2^{+}	17.1	2^{+}
17.7				17.5	2^{+}
		18.05	4^{+}	18.0	$2/4^{+}$
				19.3	4^{+}
		19.35	6^{+}		
20.0	6^{+}				
21.2	6^{+}			21.4	(6^{+})
23.6	8^{+}				
(25.0)	(8^{+})				
27.6	8^{+}				
28.8	8^{+}				
31.1	8^{+}				
32.6	8^{+}				
35.1	(10^{+})				

Also shown are the α cluster model (ACM) [4] calculations for the linear and kite (both $K=0$ and 2) configurations and cranked Nilsson-Strutinsky (CNS) (8p-8h) [5] calculations. Given the nature of the decay process, some sensitivity to 8p-8h excited states might be expected. Indeed, the lower excitation energy trend in the data appears to be well reproduced by both the ACM and CNS calculations. And given that not absolute excitation energies, but rather trends with increasing angular momenta, tend to be predicted by such

TABLE II. The grazing angular momenta, l_i, extracted from the correlation analysis.

E_{beam} (MeV)	l_i ($\pm 1\hbar$)
82–84	19.1
86–90	20.9
93–99	22.6
102–106	23.4
108–112	23.7
114–120	26.5

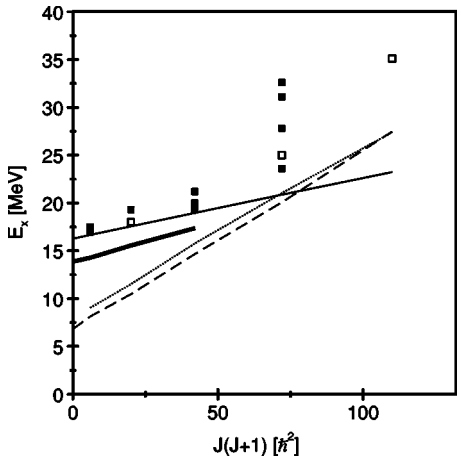

FIG. 12. The energy-spin systematics of ^{16}O excited states decaying by ^{8}Be emission, from the present data and Refs. [7,9]. The uncertain state at 25.0 MeV and tentative spin assignment for the 35.1 MeV peak are represented by the open squares. The α cluster model calculations [4] for the chain $K=0$ (solid-line), kite $K=0$ (dashed-line) and $K=2$ (dotted-line), and cranked Nilsson-Strutinsky calculations [5] for the 8p-8h configuration (bold solid-line) are indicated.

models, a displacement of the band to higher energy might indicate that the lowest-energy 8^+ states might form the continuation of the 8p-8h band. This trend may predict the existence of a 10^+ state close to 27 MeV; no evidence for such an excitation could be found in the present data. Possibly improved excitation energy resolution could allow such a resonant state to be observed.

It is also clear that several of the resonances cannot be explained by the 8p-8h bands, in particular the 8^+ states close to 32 MeV and the proposed 10^+ state at 35.1 MeV. It is possible that these are associated with the extension of bands associated with more compact configurations.

One feature which is apparent, particularly in Fig. 11, is that there are no further narrow ($\sim$1–2 MeV) resonant structures at excitation energies in excess of 36 MeV. We note that the experimental excitation energy resolution scales as $\sqrt{E_x - E_{thresh}}$, where $E_{thresh}=14.43$ MeV. Thus, the increase in the experimental contribution to the peak width between $E_x=35$ and 45 MeV is only 22%. Thus, if the states observed here are associated with rotational bands, then the bands appear to terminate at 35.1 MeV with a possible spin of 10^+.

V. SUMMARY AND CONCLUSIONS

A study of the ^{12}C(^{12}C, ^{16}O$^*\rightarrow{}^{8}$Be+^{8}Be)^{8}Be reaction has been performed with beam energies from 82 to 120 MeV. A large array of strip detectors permitted the detailed reconstruction of the reaction process, in particular the excitation energies and spins of the excited ^{16}O states. Evidence is found for excitations up to 35.1 MeV with spins of up to 10 $\hbar$. Beyond these excitation energies, no further evidence for resonances is found. The energy-spin systematics of many of the states appear to follow the trend found for 8p-8h bands in both the α cluster model and cranked Nilsson-Strutinsky calculations. However, these models do not provide a complete description, and alternative structures may describe many of the observed states. The absence of the states observed in the present measurements in the reported α-decay [15] channel would suggest that the asymptotic single-particle configurations are nevertheless 8p-8h in character. The full complexity of the ^{16}O spectrum is not revealed here, and measurements provide enhanced excitation energy resolution. This could be achieved by improvements in the precision with which the emission angles of the decay products are determined.

ACKNOWLEDGMENTS

The authors wish to thank the staff of the Department of Nuclear Physics at the Australian National University for assistance in running the experiments. We acknowledge the financial support of the U.K. Engineering and Physical Sciences Research Council (EPSRC). The experimental work was performed under a formal agreement between the EPSRC and ANU.

[1] L. R. Hafstad and E. Teller, Phys. Rev. **54**, 681 (1938).
[2] J. M. Irvine, C. D. Latorre, and V. F. E. Pucknell, Adv. Phys. **20**, 661 (1971).
[3] Y. Fujiwara *et al.*, Suppl. Prog. Theor. Phys. **68**, 29 (1980).
[4] W. Bauhoff, H. Schultheis, and R. Schultheis, Phys. Rev. C **29**, 1046 (1984).
[5] S. Aberg, I. Ragnarsson, T. Bengtsson, and R. Sheline, Nucl. Phys. **A391**, 327 (1982).
[6] A. Tohsaki, H. Horiuchi, P. Schuck, and G. Röpke, Phys. Rev. Lett. **87**, 192501 (2001).
[7] P. Chevallier, F. Scheibling, G. Goldring, I. Plesser, and M. W. Sachs, Phys. Rev. **160**, 827 (1967).
[8] A. H. Wuosmaa, Z. Phys. A **349**, 249 (1994).
[9] M. Freer *et al.*, Phys. Rev. C **51**, 1682 (1995).
[10] R. L. Cowin and D. L. Watson, Nucl. Instrum. Methods Phys. Res. A **399**, 365 (1997).
[11] C. A. Bremner *et al.*, Phys. Rev. C **66**, 034605 (2002).
[12] M. Freer, Nucl. Instrum. Methods Phys. Res. A **383**, 463 (1996).
[13] C. J. Metelko *et al.*, Phys. Rev. C **68**, 054321 (2003).
[14] S. J. Sanders, L. M. Martz, and P. D. Parker, Phys. Rev. C **20**, 1743 (1979).
[15] W. D. M. Rae, S. C. Allcock, and J. Zhang, Nucl. Phys. **A568**, 287 (1994).
[16] F. Brochard, P. Chevallier, D. Disdier, V. Rauch, G. Rudolf, and F. Scheibling, Phys. Rev. C **13**, 967 (1976).